



Effect of Media Composition and Culture Time on the Lipid Profile of the Green Microalga *Coelastrum* sp. and Its Suitability for Biofuel Production

Ruby Alejandra Valdez-Ojeda¹ · Maria Guadalupe del Rayo Serrano-Vázquez¹ · Tanit Toledano-Thompson¹ · Juan Carlos Chavarría-Hernández¹ · Luis Felipe Barahona-Pérez¹

Received: 3 September 2019 / Accepted: 21 June 2020 / Published online: 30 June 2020
© Springer Science+Business Media, LLC, part of Springer Nature 2020

Abstract

The development of biofuels as an alternative to the use of fossil fuels is growing worldwide due to environmental concerns and energy independence; thus, considerable technical progress has been achieved in biofuel production. Microalgae have been widely used for nutrient removal during wastewater treatment and produce compounds that can be used as feedstock for biofuel synthesis. In this work, the green microalga *Coelastrum* sp. was cultivated using industrial wastes: molasses as the carbon source and synthetic wastewater as the culture medium to determine the potential of its use for biofuel production. The use of synthetic wastewater (SWW) and molasses improved biomass production when compared with cultures carried out in a standard laboratory culture medium, such as tris-acetate-phosphate (TAP). Growth rates of 0.31 and 1.4 day⁻¹ were attained during exponential growth rate with SWW and molasses and TAP media, respectively. The best results in biomass and lipid content, 2.29 ± 0.05 and 0.71 ± 0.03 g L⁻¹, were obtained after 15 days of culture in SWW with molasses. The analysis of the lipid profile, produced by *Coelastrum* sp. cultured under these conditions, determined that the microalga can be considered as a high-quality feedstock for producing green diesel, bio-jet fuel, or biodiesel.

Keywords Synthetic wastewater · Molasses · Triacylglycerides · Transesterification · Algal metabolites

Introduction

Due to increasing energy independence and environmental concerns, the development of biofuels as an alternative to the use of fossil fuels is growing worldwide. Biofuels have been in use in the last decade, and research and technological development continue. They are derived from biological sources that make them a renewable source for energy production together with low greenhouse gas emissions into the atmosphere [1]. Considerable technological progress has been achieved in biofuel production; however, the sustainability aspect has emerged as an important issue in recent years. With sustainability as a goal, efforts are being made to develop production schemes based on biological wastes as feedstock to improve sustainability criteria.

Heterotrophic cultivation in microalgae presents significant biomass production advantages over the more common autotrophic method [2] but nevertheless requires an organic carbon source [3], which makes the production process economically unviable for biofuel production. In this sense, alternative and inexpensive carbon sources such as cane molasses [4] have been suggested to replace pure glucose for cultivation to support rapid growth and attain high oil yields from algae while significantly reducing production costs up to 50% [5, 6]. Molasses is a viscous and dark final effluent obtained during the preparation of sugar by repeated crystallization and is currently used as an animal feed or raw material for ethanol and other value-added chemical production [7]. Composition of molasses varies depending on the season, location, and other production variables. Regarding nutrients from molasses, 40% C and 2–6% N contents have also been reported [8]. Furthermore, an average C/N ratio in molasses of approximately 55 has been reported [9]. In Mexico, molasses is chemically constituted by sucrose (26–40%), reducing sugars (12–25%) and nitrogen (0.4–1.5%) [10]. Molasses production increased from 2006–2007 to 2015–2016 by 10.5% with 2 million tons produced per year and sold at a relatively stable price.

✉ Luis Felipe Barahona-Pérez
barahona@cicy.mx

¹ Centro de Investigación Científica de Yucatán AC, Calle 43 No. 130 x 32 y 34 Colonia Chuburná de Hidalgo., 97205 Mérida, Yucatán, Mexico

However, only few microalgae species adapt to heterotrophic cultivation [11, 12]. Thus, it is important to evaluate more fast growing and lipid-rich microalgae that can be cultivated in heterotrophic systems for biofuel production. Another course for attaining sustainability in microalgae culturing for biofuel production is the use of low-cost culture media hence the use of wastewater. Microalgae of different genera have been widely used for nutrient removal during wastewater treatment [13]. In fact, some species have shown excellent efficiency for nutrient removal [14]. Therefore, with the advent of renewable energies and GHG emissions reduction, recent studies have focused on maximizing the biomass and lipid yields of microalgae to improve its viability for biofuel production [13] and, at the same time, performing a wastewater treatment.

Among microalgae species, *Coelastrum* sp. has been proposed as a suitable feedstock for biodiesel production, with great potential for CO₂ biofixation, nutrient removal from wastewater [14], and other high-value-added products [15]. Moreover, its high lipid yield and suitable fatty acid profiles with potential for biofuel production have been reported [16] and its growth performances compared with other species [17]. It has also been reported that some microalgal species are capable of naturally produce hydrocarbons [18] and even fatty acid methyl esters (biodiesel) (FAMES) [19]. On the other hand, native algal strains are adapted to local environmental conditions and can be highly competitive and tolerant to a wide range of culture conditions [20]. In this work, the potential of a native strain of *Coelastrum* sp. was investigated for biofuel production using molasses as a carbon source in synthetic wastewater as an alternative to classic culture media. This potential was based on the production of a specific biofuel (green diesel, biodiesel, or bio-jet fuel) following the lipid profiles that resulted with changes in media composition and culture time.

Materials and Methods

Strain and Culture Conditions

Coelastrum sp. (strain UADY-PRIORI-014-FMVZ-05) was kindly provided by the Facultad de Medicina Veterinaria y Zootecnia of the Universidad Autónoma de Yucatán in Yucatan, Mexico, and characterized genetically and morphotaxonomically in our laboratory [21].

Growth cultures were carried out in 500-mL Celstir flasks with mechanical agitation using synthetic wastewater (SWW) employed in heterotrophic cultivation of *Chlorella vulgaris* [2], modified in the present study to simulate the composition of domestic wastewater, containing the following compounds (mg L⁻¹): NaCl, 7; CaCl₂, 2; MgSO₄ 7H₂O, 1; K₂HPO₄, 100; KH₂PO₄, 50; Na₂HPO₄, 30; and NH₄Cl, 192. This means 50.2 g/L of N in the medium. Industrial molasses was sent to an external laboratory to determine its proximate

composition according to AOAC 1908 methodology and the official Mexican norms (NMX-317-S-1978; NMX-F-428-1982). Molasses was added as a carbon source in the SWW at 10% v/v, according to previous studies carried out in our group [22]. The elemental composition of molasses (4 mg) was performed in a Thermo Scientific Elemental Analyzer Flash 2000 to calculate the C/N ratio. Tris-acetate-phosphate (TAP) medium was used as a reference culture [23]. Nitrogen limitation in TAP and SWW media was performed for comparison purposes with the omission of NH₄Cl from Hutner's solution but still maintaining the Mo₇O₂₄ (NH₄)₆·4H₂O content (0.011 mg L⁻¹ nitrogen, in TAP medium) [24]. The media pH was adjusted to 7 with 1 M HCl or KOH and sterilized for 20 min at 120 °C and 1.1 bar. Growth curves with 540,000 cells mL⁻¹ as inoculum were carried out. Growth conditions were 25 ± 2 °C, 16:8 h photoperiod (light:dark), 30 μmol m⁻² s⁻¹ light intensity, and 120 rpm agitation. Microalgae cell growth was evaluated by measuring the culture cell concentration with a Neubauer hemocytometer.

Specific Growth Rate Determination

Growth curves of the microalga were created by plotting the cell concentration against culture time from daily 1 mL sampling. The exponential growth phase was visually determined as a straight line during the growth phase. Cell concentration (cells mL⁻¹) and time (d) values were substituted into Eq. (1) to obtain the specific growth rate μ (d⁻¹).

$$\mu = \frac{\ln \frac{C_2}{C_1}}{t_2 - t_1} \quad (1)$$

where C₂ and C₁ are the culture cell concentrations at t₂ (end of exponential growth phase time) and t₁ (beginning of the exponential growth phase), respectively [25].

Biomass Recovery and Lipid Extraction

The lipid profiles were analyzed at three points during the culture period: at days 5 (TAP5 and SWW5) and 15 of culturing (TAP15 and SWW15) and at 15 days of nitrogen limitation in TAP medium (TAP15-N) for comparison purposes. At each sampling point, cell biomass was recovered (centrifugation at 5000 rpm at 4 for 10 min). The pellet was rinsed (3×) with distilled water to eliminate media remnants. The washed biomass was cooled to -8 °C for 24 h and vacuum freeze-dried for 72 h.

Lipid extraction was carried out by solvent extraction based on [26] and modified as described below [27]. The dry biomass collected was poured into 30 mL of 2:1 v/v chloroform:methanol mixture and incubated at 38 °C for 3 h

with agitation at 150 rpm. The extracted biomass was separated from the organic extract and extracted four more times until the absence of organic compounds was confirmed by thin layer chromatography. All organic extracts were combined, and the solvent mixture was eliminated by vacuum evaporation.

Statistical Analysis

All cultures were conducted in triplicate ($n = 3$). For statistical analysis, the t Student test was performed with the Origin@ 9.1 data analysis and graphing software (OriginLab Corporation, Northampton, MA). Significance level was 0.05.

Lipid Profile Characterization

The lipid extract (0.2 g) was partitioned in a 30×2 -cm high-purity silica gel 60, 70–230 mesh (Sigma-Aldrich, USA) chromatographic column. A gradient elution was performed using hexane and ethyl acetate as the mobile phase as follows: pure hexane, then hexane:ethyl acetate solvent mixtures of 9:1, 8:2, and 7:3 v/v, pure ethyl acetate, and finally, pure methanol. All solvents were of analytical grade (Baker, Mexico). The elution of the lipid compounds from the column was monitored by thin layer chromatography. When compounds stopped eluting from the column, a more polar mobile phase was used. Thin layer chromatography was carried out on TLC silica gel 60 F₂₅₄ aluminum foil plates (Merck, Germany), and a mixture of hexane:ethyl acetate:acetic acid (9:1:0.1 v/v) was utilized as the mobile phase. The plates were developed by immersion in a phosphomolybdic acid solution followed by moderate heating. Fractions obtained from column chromatography were classified following the nature of the compounds they contained. The fractions containing triacylglycerides were transesterified by homogeneous alkaline catalysis [21] to obtain the FAME derivatives. Fractions containing hydrocarbons, FAME, terpenes, and free fatty acids were analyzed on an Agilent 6890 N gas chromatograph equipped with an Agilent 5975B mass selective detector. Compounds were separated on a $30 \text{ m} \times 0.25 \text{ mm ID} \times 0.5\text{-}\mu\text{m}$ film thickness Agilent HP-5 MS UI capillary column, and the carrier gas was He at 3 mL min^{-1} . The temperature conditions were $70 \text{ }^\circ\text{C}$ for 5 min, a $10 \text{ }^\circ\text{C min}^{-1}$ ramp to $200 \text{ }^\circ\text{C}$, a $20 \text{ }^\circ\text{C min}^{-1}$ ramp to $290 \text{ }^\circ\text{C}$, and a $10 \text{ }^\circ\text{C min}^{-1}$ ramp to $300 \text{ }^\circ\text{C}$, which was maintained for 22 min. The ionization voltage was 70 eV, and the sample injection volume was $1 \mu\text{L}$. The identification of the compounds was carried out taking into account a match level of $\geq 90\%$ with the NIST library provided with the equipment software and a peak area $\geq 4\%$ of the total area of each sample.

The polar fractions containing phospholipids were analyzed by attenuated total reflection FT-IR spectroscopy. Spectra were acquired with a Tensor II FT-IR spectrometer (Bruker Optics,

Germany) fitted with an ATR accessory. The transmittance spectra were collected between 4000 and 500 cm^{-1} at a spectral resolution of 4 cm^{-1} with 32 scans coadded and averaged. The samples were analyzed without prior treatment.

Estimation of Physico-chemical Parameters to Assess Potential of *Coelastum* sp. Lipids as Feedstock for Biofuel Production

The compounds identified in the lipid extracts were grouped into five fractions according to their potential to be used as raw material for its transformation into renewable fuels, or their potential to be used directly as fuel without requiring to be processed. Heterogeneous catalysis transformation processes such as hydrodeoxygenation, hydroisomerization, and hydrocracking were considered in the analysis. The oxygen weight percent in the fractions containing this element, as well as the H/C atomic ratio, was calculated as parameters to assess the usability of the different fractions in the mentioned biofuel-obtaining processes.

On the other hand, for the transesterifiable fractions, the potential quality of biodiesel was estimated considering that (a) after transesterification, the FAMES obtained conserve the aliphatic structure of the components in the raw material, and (b) the properties of the biodiesel obtained can be estimated from the proportion of individual FAMES in the mixture. The methodology used to estimate the properties of biodiesel is described below.

Property data for pure fatty esters considered in the samples was gathered from experimental reports or calculated from correlations reported in literature as indicated in Table 1. Using this information in combination with the Kay's mixing rule (Eq. (2)), density at $15 \text{ }^\circ\text{C}$ (ρ), kinematic viscosity at $40 \text{ }^\circ\text{C}$ (ν), higher heating value (HHV), and iodine value (IV) were estimated for biodiesels. For the case of cetane number (CN), cold filter plugging point (CFPP), and oxidative stability (OSI), selected correlations taken from the literature were applied. In total, seven main fuel properties of biodiesel were estimated and compared with the corresponding standard limits when applicable.

$$f_B = \sum_{i=1}^n x_i \cdot f_i \quad (2)$$

The use of Eq. (2) is justified for predicting biodiesel properties, given that they are simple mixtures constituted generally by less than 10 single compounds of the same family, thus having similar physicochemical properties. In this equation, f was replaced by ρ , CN, $\ln \nu$, HHV, or IV, depending on the property to be estimated. Subscript i refers to individual i th fatty ester and subscript B refers to the mixture of esters or biodiesel, n is the number of fatty esters in the mixture, and x represents their weigh fractions.

Table 1 Pure component data of methyl esters for biodiesel property estimation

Ester property	ρ @15 °C (kg/m ³)	b ^a (kg/m ³ K)	a ^a (kg/m ³)	ν @40 °C (mm ² /s)	HHV (MJ/kg)	IV ^j g I/100 g biodiesel
C16:0	869.4 ^f	-0.7438	1083.7	4.38 ^e	39.45 ^h	0.0
C16:1	872.8 ^b	-	-	3.06 ^b	39.29 ^h	94.5
C16:2	891.5 ^c	-	-	3.05 ^d	39.04 ⁱ	190.5
C16:3	902.9 ^c	-	-	2.60 ^d	38.78 ⁱ	288.0
C18:0	867.8 ^f	-0.7209	1075.5	5.85 ^e	40.07 ^h	0.0
C18:1	877.7 ^g	-	-	4.51 ^e	39.91 ^h	85.6
C18:2	889.9 ^g	-	-	3.65 ^e	39.70 ^h	172.4

^a Parameter of Eq. (3) for calculation of density as a function of temperature

^b [32]

^c Calculated with Eq. (4), provided by [29]

^d Calculated with Eq. (5), provided by [29]

^e [32]

^f Calculated using Eq. (3) [28]

^g [28]

^h [33] Method: modification of ASTM D240 and D2015

ⁱ Calculated with Eq. (6), [38]

^j Calculated with Eq. (7), [31]

Density of some FAMES was estimated by using Eq. (3) proposed by Pratas et al. [28], where a and b are fitted parameters which values are given in Table 1.

$$\rho \left[\frac{\text{kg}}{\text{m}^3} \right] = b \cdot T[\text{K}] + a \quad (3)$$

Some other FAME densities are calculated with Eq. (4) proposed by Ramírez [29]. Dynamic viscosity (ν) [29], higher heating value (HHV) [30], and iodine value (IV) [31] of certain individual FAMES were calculated with Eqs. (5–7) and data from other studies [32–34] as indicated in Table 1. In Eqs. (4–7), M is the molecular weight, N is the number of double bonds, and T is the temperature in K. ρ in Eq. (4) is given in kg·m⁻³, ν in Eq. (5) is in mPa·s, the units of HHV in Eq. (6) are MJ kg⁻¹, while those of IV are g I/100 g biodiesel.

$$\rho = 1.069 + \frac{3.575}{M} + 0.0113 \cdot N - 7.41 \cdot 10^{-4} \cdot T \quad (4)$$

$$\ln(\nu) = -18.354 + 2.362 \cdot \ln(M) - 0.127 \cdot N + \frac{2009}{T} \quad (5)$$

$$\text{HHV} = 46.19 - \frac{1794}{M} - 0.21 \cdot N \quad (6)$$

$$\text{IV} = 100 \cdot \frac{253.81 \cdot N}{M} \quad (7)$$

The cetane number of biodiesels (CN) was calculated by using Eqs. (8–10) proposed by Mishra et al. [35]. To estimate the CFPP, Eq. (11) reported by Serrano et al. [36] was used. In

this equation, SAT_{C16-C24} are the weight percent of saturated C16-C24 FAMES. Finally, the OSI value was estimated by using Eq. (12) proposed by Park et al. [37], where X is the sum of the weight percent of the linoleic and linolenic FAMES, while Y is the oxidative stability, in h.

$$\text{CN} = 63.41 - (0.0728 \cdot \text{DU}_m) + (0.03495 \cdot \text{SCSF}) - (3.26 \cdot 10^{-4} \cdot \text{DU}_m \cdot \text{SCSF}) \quad (8)$$

where

$$\begin{aligned} \text{DU}_m = & (\text{monounsaturated } C_n : 1, \text{ wt}\%) \\ & + 2(\text{polyunsaturated } C_n : 2, \text{ wt}\%) \\ & + 3(\text{polyunsaturated } C_n : 3, \text{ wt}\%) \end{aligned} \quad (9)$$

and,

$$\text{SCSF} = \frac{1}{100} \sum (\text{MW}_i \cdot \text{wt}\% \text{ of saturated methyl esters}) \quad (10)$$

$$\text{CFPP}(\text{°C}) = -26 + 5.76[\text{SAT}_{\text{C16-C24}}]^{0.5} \quad (11)$$

$$Y = \frac{117.9295}{X} + 2.5905 \quad (12)$$

Results and Discussion

Coelastrum sp. Growth in SWW

The proximate composition of molasses used in this study was as follows: humidity (26.22%), soluble solids (1.46°Bx), nitrogen (0.48%), protein (3.01%), crude fiber (0.63%), ash (6.42%), and total sugars (58.69%). Nitrogen and sugar contents were consistent with values reported for industrial molasses in Mexico [10] and China [7]. Meanwhile, the elemental composition analysis indicated contents of C, H, N, and S of 43.54, 6.28, 0.66, and 0.28%, respectively. With these results, a C/N ratio in molasses added with synthetic wastewater of 70.3 was calculated. This value is high, considering that in the case of wastewaters added with carbon sources, C/N ratios of 5 to 30 have been reported [38, 39]. Total sugars in molasses are mainly (two-thirds) constituted by sucrose, which is difficult to assimilate by microalgae. If reducing sugars present in molasses are considered as the main carbon source, then a C/N ratio of 13.1 can be considered for this study. C/N ratios above 20 favored cell lipids content in *Chlorella sorokiniana* [40]. Studies in our laboratories are currently being carried out to exactly determine the amount of carbon source available for microalgae in pretreated molasses.

Coelastrum sp. cultured in SWW with molasses as the carbon source showed continuous growth ($\mu = 0.31 \text{ day}^{-1}$) until day 13 of culturing, when the cell concentration began to decline. In TAP medium, *Coelastrum* sp. showed 1 day of lag phase (Fig. 1), then 1 day of exponential growth ($\mu = 1.4 \text{ day}^{-1}$), and entered the stationary phase until the end of culturing. Specific growth rates of 0.23 and 0.47 day^{-1} have been reported for *Coelastrum* sp. cultured in BG11 medium [14] and *Chlorella vulgaris* cultured with glucose-galactose as carbon source [3], respectively. Despite the use of a complex carbon source in this study, cultures did not show growth inhibition; on the other hand, the sustained longer growth period in SWW was probably due to the use of carbohydrates as a carbon source, as reported by Yan et al. [5] with the

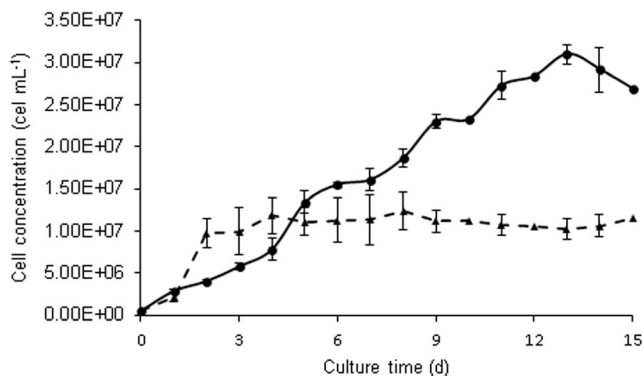


Fig. 1 Growth curves of the microalga *Coelastrum* sp. in TAP medium (▲) and synthetic wastewater combined with molasses (●). Data showed as mean \pm standard error ($n = 3$)

microalga *Chlorella protothecoides*, which make this medium very attractive for microalgal biomass production. The higher growth rate in TAP medium can be due to the better availability of a carbon source (acetate) for the microalga in this medium than in SWW complemented with molasses (glucose, fructose, and sucrose). It has been reported that the use of Na-acetate as a carbon source produced better growth of *Chlorella vulgaris* in SWW than that seen with glucose or sucrose [41]. In this work, the maintained growth of *Coelastrum* sp. in SWW with molasses could be explained by a high availability of nitrogen. The addition of molasses to SWW increased the nitrogen content, from that present in TAP medium, by 7 times. Nitrogen contents used by Mousavi et al. [14] were 48 to 80 mg L^{-1} whereas in this study, nitrogen concentration was 768 mg L^{-1} most of nitrogen coming from molasses. Optimization of these parameters is needed. Productivity parameters analyzed at different sampling points (Table 2) indicated that *Coelastrum* sp. produced more biomass (dry basis) when cultured in SWW and molasses than when cultured in TAP medium. After 15 days of culture in SWW complemented with molasses, $2.29 \pm 0.05 \text{ g L}^{-1}$ of dry biomass were attained. This value is lower than that (8.8 g L^{-1}) obtained by Yan et al. [5] with untreated molasses but close to 2.24 g L^{-1} reported by Abreu et al. [3]. Concerning lipid production, 0.71 g L^{-1} was attained when *Coelastrum* sp. was cultivated in SWW with molasses, and increased to 0.82 g L^{-1} after nitrogen limitation was applied to the culture at the end of the exponential growth phase. Rai and Gupta [42] have reported lipid production values from 0.092 to 0.36 g L^{-1} with *Scenedesmus abundans* cultured in different media. In another study, Gao et al. [39] reported lipid production values from 0.025 to 0.32 g L^{-1} when *Chlorella* sp. was cultured under different carbon and nitrogen concentrations in culture media. Biomass and lipid production varied between treatments indicating a strong effect of culture conditions on these parameters. Higher lipid contents were detected when the microalgae were cultured in batch mode for 15 days. The nitrogen limitation stage enhanced biomass production only while lipid content began to decrease. It has been reported that if sufficient nitrogen is stored within the cells in the growth phase when the nitrogen amount is abundant, it can be metabolized during nitrogen depletion, resulting in more microalgal growth instead of lipid production [43]. The increase in growth with molasses as a carbon source has been documented in *Chlorella vulgaris*, *Scenedesmus obliquus* [44], and *Chlorella pyrenoidosa* [4].

Nitrogen limitation showed a more noticeable effect on growth than lipid production when *Coelastrum* sp. was cultivated in TAP medium (Fig. 2). It can be seen that the increase in cell weight is not due to lipid production enhancement. An explanation to this behavior could be the accumulation of starch. It has been reported that nutrient limitation can be used as a strategy to accumulate starch and lipids in microalgae

Table 2 Dry biomass, lipid production, and lipid content of *Coelastrum* sp. cultivated in TAP and SWW media at different culture times

Culture	Dry biomass weight (g·L ⁻¹)	Lipid production (g·L ⁻¹)	Lipid content ^a (%)
TAP5	0.67 ± 0.01 a,b	0.19 ± 0.01 a	28
TAP15	0.70 ± 0.03 a,b	0.23 ± 0.01 a	33
TAP-15 N	1.29 ± 0.09 c,d	0.32 ± 0.01 a,b	25
SWW5	1.67 ± 0.17 d	0.39 ± 0.08 a,b	23
SWW15	2.29 ± 0.05 e	0.71 ± 0.03 a,b	31
SWW15-N	4.17 ± 0.42 f	0.82 ± 0.08 b,c	20

Data are expressed as mean ± standard error. Different letters represent significant differences (*t* test, *p* < 0.05)

^aBased on dry biomass, w/w

[45]. However, regulating the distribution of these energy-containing compounds is not clear, as it depends on several environmental conditions [46]. Further investigation is needed to explain why the cells stop accumulating lipids while growth continue.

Coelastrum sp. Lipid Profiles

The crude extracts from all cultures were partitioned by gravity column chromatography to obtain fractions that were classified according to the type of compounds in them (from non-polar to polar compounds). Five fractions were obtained from each crude extract: the first fraction was the least polar and contained mainly hydrocarbons. The second fraction was mainly composed of triacylglycerides. The third fraction contained sterols, free fatty acids, and fatty alcohols; the fourth fraction was constituted mainly by terpenes, and the more polar fifth fraction corresponded to phospholipids. The fraction containing triacylglycerides was transesterified before GC-MS analysis. As expected, the composition of the crude extracts varied with culture conditions, as shown in Fig. 3.

After 15 days of culturing *Coelastrum* sp. in batch mode in TAP medium, hydrocarbons were approximately 3% of the total lipid extract. When nitrogen limitation was applied to the culture, the presence of hydrocarbons became more prominent (22% of total lipid extract). In SWW-molasses medium,

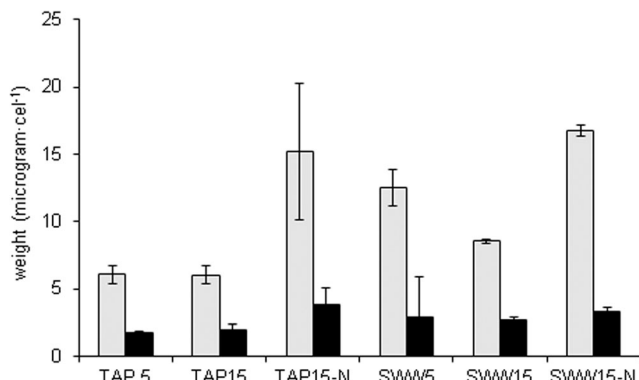


Fig. 2 Cellular dry biomass (gray bar) and cellular lipid content (black bar) of *Coelastrum* sp. cultivated in TAP and synthetic wastewater combined with molasses. Data showed as mean ± standard error (*n* = 3)

Coelastrum sp. showed the same production of hydrocarbons (3% of the total crude extract) at 5 and 15 days of culture. After nitrogen limitation, hydrocarbons were 4% of the total crude extract, showing little effect. The contribution of triacylglycerides to the total crude extract at the end of the exponential growth phase in TAP medium was 6% and remained almost the same after 15 days of culture or after nitrogen limitation (6 and 9%, respectively). When *Coelastrum* sp. was cultivated in SWW-molasses medium, 16% was the contribution of triacylglycerides to the total lipid extract. It increased to 55% after 15 days of culture in batch mode and to 48% after nitrogen limitation. These results indicate that triacylglycerides were the compounds that *Coelastrum* sp. produced after the exponential growth. In the case of sterols, their highest contribution to total microalgal extract was attained at the end of the exponential growth phase (3.9% and 5.3% for TAP and SWW-molasses media, respectively). Sterols are structural compounds of cell membranes and are mainly synthesized during cell multiplication [47]. Their presence decreased as other compounds were produced within the cells during the stationary phase. Terpenes are secondary metabolites that are mainly produced after the exponential growth phase [48]. In the case of *Coelastrum* sp., the contribution of terpenes to the crude extract at the end of the exponential growth phase was 11.7% and 8.11% (in TAP and

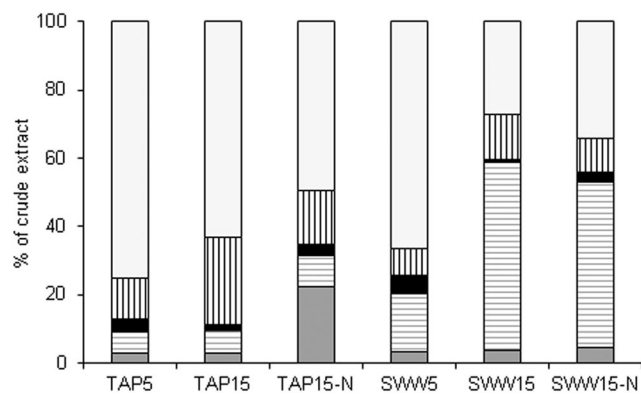


Fig. 3 Lipid distribution of the microalgae *Coelastrum* sp. at different times and culture media. Hydrocarbons (dark gray bars); triacylglycerides (horizontal lines); sterols (black bars); terpenes (vertical lines); and phospholipids (light gray bars)

SWW-molasses, respectively). After 15 days of culture in batch mode, terpenes increased to 25% in TAP medium and only 13% in SWW-molasses. Values of terpene content after nitrogen limitation decreased to 15.8% in TAP medium and 10.1% in SWW-molasses medium. An explanation of this behavior is beyond the scope of this study. The contribution of the phospholipidic fraction to the total extract was the most important after the exponential growth phase in both TAP and SWW-molasses media (75 and 66%, respectively) probably because cells were multiplying and mainly producing cell wall phospholipids. Their contribution decreased after 15 days of culture in TAP and SWW-molasses media to 63 and 27%, respectively, as secondary metabolites were produced. After nitrogen limitation, changes on the phospholipid contribution to the total lipid extract were minimal. From a production process point of view, what is important is the amount of the compound of interest that can be attained. The yield of each fraction in 1 L of culture media is shown in Fig. 4. If triacylglycerides are the fraction of interest, *Coelastrum* sp. can be cultivated in SWW-molasses medium in batch mode for 15 days (avoiding the addition of more nutrients), as nitrogen limitation had almost the same effect.

Lipid Identification in *Coelastrum* sp. Cultures

Fifty-three compounds were identified by GC-MS from the first four fractions that eluted from the silica gel column (Table 3). The fifth fraction (phospholipids) was only analyzed by FT-IR to corroborate the presence of the P-O-C band. In this section, the profile of the lipids produced by *Coelastrum* sp. is discussed with the exception of the phospholipidic fraction, which was not fully identified. When *Coelastrum* sp. was cultivated in TAP medium, the hydrocarbon 1-docosene and the sterol chondrillasterol were the most abundant compounds at the end of the exponential growth phase. After 10 more days in batch mode culturing, 1-docosene was 6 times less abundant, chondrillasterol was not

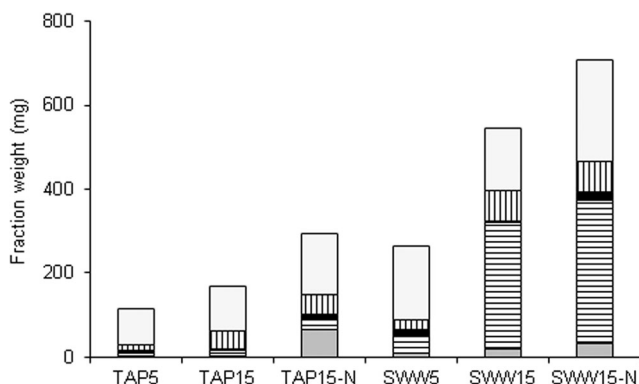


Fig. 4 Yield of the lipid extract fractions of the microalgae *Coelastrum* sp. at different times from 1 L of culture media. Hydrocarbons (dark gray bars); triacylglycerides (horizontal lines); sterols (black bars); terpenes (vertical lines); and phospholipids (light gray bars)

detected, and the production of TAGs was favored. The most abundant fatty acid methyl esters (FAMES) detected at this point were C18:1 and C18:2 with smaller amounts of C16:0, C16:2, and C16:3. Neophytadiene was also as abundant as C18 FAMES. Phytol was also detected but in smaller quantities than neophytadiene. Although nitrogen limitation in TAP medium did not induce more production of TAGs than that in batch mode, the FAME profile changed; more C16:0 was present, and the production of the (Z) isomer of C18:1 (the most abundant FAME) was observed.

When SWW-molasses was the culture medium, *Coelastrum* sp. mainly produced TAGs during the first 5 days of culturing, showing the presence of C18:1 (the E isomer) and C16:0 as the main FAMES. The production of more TAGs compared with that of the TAP medium during this period can be due to the slow growth of *Coelastrum* sp. in SWW-molasses that allows for the production of some reserve compounds. After 10 more days in batch mode culturing, the production of TAGs was improved, but the FAME profile was almost the same. This indicates that the metabolism during this period was the same that occurred during the first 5 days of slow growth, resulting in TAG accumulation. Elimination of nitrogen from SWW did not enhance the accumulation of TAGs from what was accumulated in batch mode. The more abundant FAMES were C16:0, C18:0, and C16:1, which indicates a possible shift towards more saturated TAG production. The nitrogen limitation experiment with SWW cannot be considered a complete limitation as in the case of the TAP medium. This is because the addition of molasses as a carbon source at the beginning of the limitation phase also introduced the addition of nitrogen contained in the molasses. More work is underway to evaluate the effect of the nitrogen contained in the molasses.

As expected, the FT-IR spectra of the phospholipidic fractions from all experiments showed similar patterns (Fig. 5). A strong signal at 1035 cm^{-1} characteristic of symmetric P-O-C bond stretching can be observed. The bands at 1095 and 1240 cm^{-1} are associated with the symmetric/asymmetric bond stretching of a PO_2^- diester from the phosphate group [49]. Bands at 1458 , 1715 , and $2852\text{--}2915\text{ cm}^{-1}$ are characteristic of the CH_2 , C=O , and C-H groups, respectively. Although the phospholipidic fractions were not fully identified, phosphatidylglycerol (PG) and phosphatidylcholine (PC) have been reported in *Scenedesmus* sp. lipid extracts in a more detailed study carried out by Yao et al. [47].

Potential of *Coelastrum* sp. Lipids for Biofuel Production

The compounds present in the lipid extracts were grouped into 5 fractions as indicated in Table 4, and a qualitative assessment of the potential use of each fraction as a feedstock for obtaining renewable liquid fuels was estimated. In this table,

Table 3 Compounds identified in lipid extracts of the green microalga *Coelastrum* sp.

Peak	Compound	% of total peak area					
		TAP5	TAP15	TAP15-N	SWW5	SWW15	SWW15-N
1	1-Octadecene	2.6					
2	Octadecane		0.7		0.6		
3	Eicosane				0.8		
4	Heneicosane				0.5		
5	Hexacosane	1.7					
6	Nonadecene			3.6	0.1		0.2
7	Cyclotetracosane			4.7		4.4	
8	Nonadecane				0.5		
9	1-Heptacosene			1.0	5.3	6.4	2.8
10	2,3,5-trimethyldecane		0.7				
11	Heptadecane	3.5	1.6				
12	1-Docosene	36.6	6.7				
13	17-Pentatriacontene		1.4				
14	1-Hexacosene	5.0					
15	Cyclotriacontane	1.9					
16	1-Nonacosene			5.4			0.3
17	Cyclododecane			1.9			
18	Cyclotetradecane			1.0			
19	7,10-Hexadecadienoic acid, methyl ester		3.8			3.0	4.0
20	(Z)-9-Hexadecenoic acid, methyl ester				4.8	4.2	10.8
21	Hexadecanoic acid, methyl ester		4.6	14.3	16.1	15.3	37.3
22	(Z)-9-Octadecenoic acid, methyl ester			43.4			
23	Octadecanoic acid, methyl ester			3.8	3.7	4.3	13.1
24	Octacosanoic acid, methyl ester				8.8		6.3
25	Propanoic acid, 2-methyl-, 3-hydroxi-2,2,4-trimethylpentyl ester	3.0					
26	Hexanedioic acid, bis(2-ethylhexyl) ester		5.3				
27	(Z)-7-Hexadecenoic acid, methyl ester			3.3			
28	7,10,13-hexadecatrienoic acid, methyl ester		3.7				
29	(Z)-9-(Z)-12-Octadecadienoic acid, methyl ester		3.5	12.4		13.7	18.5
30	9,12-Octadecadienoic acid, methyl ester (isomer)		15.8				
31	Butanoic acid, butyl ester		0.9				
32	(E)-9-(Z)-11-Octadecadienoic acid, methyl ester	3.1					
33	(E)-13-Octadecenoic acid, methyl ester	5.7					
34	7-Octadecenoic acid, methyl ester					40.7	
35	(E)-9-Octadecenoic acid, methyl ester		19.7		52.4		
36	Stigmasta-7,16-dien-3-ol, (3- β , 5- α)				5.7		
37	6,10,14-Trimetil-2-pentadecanone	1.8					
38	Hexadecanoic acid	1.9	1.5				
39	1-Hexadecanol		0.4				
40	1-Heptadecanol		0.5				
41	Butyl citrate		2.1				
42	1-Docosanol		0.7				
43	Ergost-7-en-3-ol, (3- β)-		2.9				
44	Triacetyl acetate	6.3				2.9	1.4
45	Ergost-7-en-3-ol	4.7					
46	Chondrillasterol	19.9					

Table 3 (continued)

Peak	Compound	% of total peak area					
		TAP5	TAP15	TAP15-N	SWW5	SWW15	SWW15-N
47	Heptacosyl acetate						1.9
48	Neophytadiene	2.2	18.5	2.4		0.2	0.7
49	Squalene				0.6	5.0	2.6
50	Phytol		5.1	2.9			0.1

the letter H, for example, indicates that this fraction has high potential to be transformed into a biofuel, meaning that it constitutes a high-quality raw material to be processed through the technology indicated in the last column of the table. In addition, the main product or products that would be obtained with this technology are indicated.

Fraction 1 corresponds to branched- and cyclo-alkanes containing between 12 and 14 C atoms without the presence of double bonds or oxygen atoms. The compounds of this fraction correspond to a renewable fuel for aviation (bio-jet fuel). Because the freezing point is one of the most critical specifications for aviation fuel ($-47\text{ }^{\circ}\text{C}$ according to ASTM D7566), the presence of molecules with sufficiently low freezing points is required. In particular, branched alkanes or isoalkanes have lower freezing points for a higher number of branches. Figure 6, generated with data from the NIST Standard Reference Database [50], shows the melting points of some linear and branched alkanes that are within the jet fuel range (C8–C16). Cyclic alkanes are also useful as aviation fuel. Moreover, a maximum of 25% content of aromatic compounds is also desirable to prevent fuel seals in ducts, connections, and containers where the jet fuel is stored. According to these criteria, fraction 1 can be used directly as bio-jet fuel

because it contains compounds in the proper range of C atoms and does not have oxygen or the presence of double bonds. In particular, fraction 1 of the TAP15 treatment is formed by tri-branched structures, which are highly desirable for aviation fuel.

Fraction 2 is composed of saturated and unsaturated linear hydrocarbons containing between 17 and 21 C atoms. These molecules are in the range of diesel fuel, which in this case is known as green diesel or renewable diesel. This fuel requires linear alkanes with medium-chain length, which provide a high cetane number. For example, n-C16, also known as cetane, has a cetane number of 100. On the other hand, chain branching reduces the cetane number but improves its cold flow properties. For this reason, a moderate percentage of mono-branched molecules is desirable. Once the olefins present are saturated, the product corresponds to a diesel with a very high cetane number. However, it is required that some molecules are transformed to branched structures to improve their cold flow properties. Both the saturation of the double bonds and the required isomerization can be carried out simultaneously in a single catalytic step referred to as hydroisomerization [51]. Moreover, the H/C values for this fraction range from 1.9 to 2.1. As a reference, alkanes containing between 17 and 21 C atoms have an average H/C ratio of 2.1. This indicates moderate levels of unsaturation, and that moderate hydrogen consumption is required to obtain the saturated product. According to the above, fraction 2 for all of the treatments constitutes a high-quality feedstock for transformation into green diesel.

The composition of fraction 3 is similar to that of fraction 2, but fraction 3 is constituted by larger molecules (C22–C35). Similarly, the double bonds present in these molecules must be saturated, and they must be isomerized to form branched structures. Additionally, molecules of this fraction must be fragmented to obtain smaller molecules. As a result of this process, bio-jet fuel and green diesel can be obtained. The levels of unsaturation for these fractions are also relatively low, with H/C atomic ratios between 1.8 and 2.0. Therefore, in this case, it is required to simultaneously perform hydroisomerization and hydrocracking reactions. Sometimes, this process is referred to as hydroconversion.

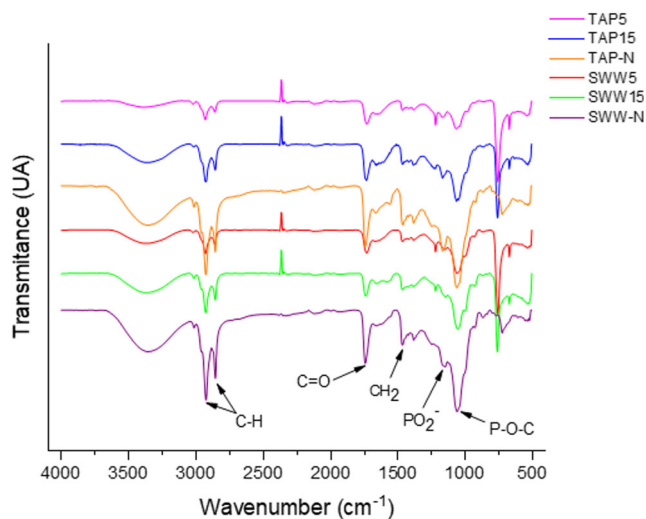
**Fig. 5** FT-IR spectra of polar fractions from *Coelastrum* sp. lipid extracts

Table 4 Fractions from lipid extracts and their estimated potential applicability for obtaining biofuels

Fraction	General description	C range	TAP5	TAP15	TAP15-N	SWW5	SWW15	SWW15-N	Product	Process
1	Branched and cyclic saturated HC	C ₁₂ -C ₁₄		H	M				BJ	none
2	Linear paraffins and olefins	C ₁₇ -C ₂₁	H	H	H	H	H	H	GD	HI
3	Linear olefins, cyclic, and paraffins	C ₂₂ -C ₃₅	H	H	H	H	H	H	BJ + GD	HI + HC
4	Oxygenated compounds	C ₈ -C ₃₂	H	H	H	H	H	H	BJ + GD	HEFA
5	Saturated and unsaturated TG and FFA	C ₁₆ -C ₁₈	H	M	H	H	H	M	BD	E-T

HC hydrocarbons, TG triglycerides, FFA free fatty acids, H high quality, M medium quality, BJ bio-jet fuel, GD green diesel, BD biodiesel, HI hydroisomerization, HC hydrocracking, E-T esterification + transesterification, HEFA hydrotreatment process for obtaining bio-jet fuel and green diesel

These transformations can be carried out in a single reaction step by using heterogeneous catalysts [52]. According to this analysis, fraction 3 constitutes a high-quality raw material with potential for transformation into bio-jet fuel and green diesel.

Fraction 4 contains oxygenated compounds containing between 8 and 32 C atoms. These compounds include alcohols of different lengths, short chain FAMES, and terpenes, among others. In addition to the hydrogenation, isomerization, and cracking reactions described for fraction 3, a hydrodeoxygenation process to eliminate the oxygen in the molecules in this fraction is required. Moreover, the values obtained for the atomic H/C ratio and the percentage by weight of oxygen are more favorable than those corresponding to the *Jatropha curcas* oil (JCO) taken as a reference [53], which values are 1.8 and 11 wt%, respectively. According to the above, fraction 4 constitutes a feed that can be transformed through the process known as HEFA [54], which is carried out in the presence of hydrogen in two reaction stages. In the first reaction step, oxygen is eliminated in the form of H₂O, CO₂, and CO, while the double bonds are saturated. In the second reaction step, isomerization and cracking reactions take place, giving rise to bio-jet fuel and green diesel as main products.

Fraction 5 corresponds to TG and FFA transformable into biodiesel. Based on their lipid profile, seven critical properties were estimated, whose values are shown in Table 5. In this table, minimum and maximum limits considered by the

American (ASTM 6751) and European standards (EN 14214) have been included when applicable. The results indicate that all biodiesels meet the American and European standards for density, cetane number, and viscosity. In addition, all comply with the OSI values of the American standard, and the SWW15-N treatment also complies with the European standard for this parameter. Regarding IV, only TAP15 treatment biodiesel fails to comply with the maximum limit established in the European standard. This is explained by its high content of polyunsaturated FAMES, which amounts to 51% approximately. With respect to the HHV, all of the biodiesels present typical values, very close to 40 MJ/kg. Finally, except for SWW15-N treatment, the rest of the biodiesels present acceptable values of CFPP, especially for temperate climates. The high content of saturated FAMES (approximately 60%) is the cause of the 18.7 °C value estimated for SWW15-N treatment biodiesel. According to the above, biodiesels from TAP15 and SWW15-N treatments were classified as medium quality, while the rest of them were of high quality, as indicated in Table 4.

Conclusions

Time and culture media showed an influence on biomass and lipid production. The culturing of *Coelastrum* sp. in synthetic wastewater complemented with molasses proved to be a good option for the production of biomass $2.29 \pm 0.05 \text{ g L}^{-1}$, and lipids $0.71 \pm 0.03 \text{ g L}^{-1}$ compared with a synthetic laboratory medium. In these conditions, an additional nitrogen limitation phase did not improved lipid production. The lipid profiles were also affected by these variables. Cultures with TAP medium showed high contents of phospholipids (more than 50% of total lipid production) which are not a good feedstock for biofuel production as the phosphate group could damage catalysts used in biofuels synthesis. SWW complemented with molasses-induced triacylglyceride production to attain up to 50% of crude lipid extract, w/w, after 15 days of culture. These compounds are the feedstock for biodiesel, green diesel, or bio-jet fuel. Moreover, the nature of the triacylglycerides produced by *Coelastrum* sp. can produce high-quality

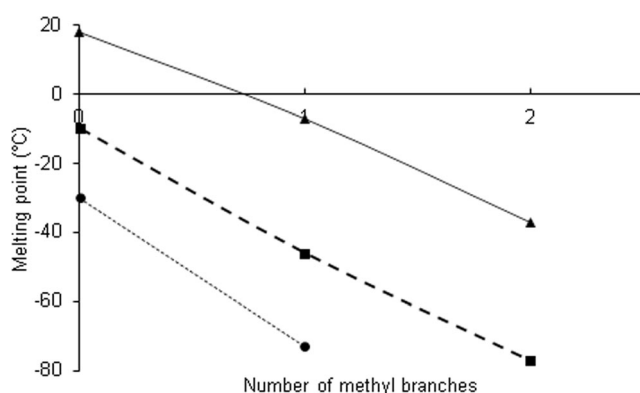


Fig. 6 Melting points of C₁₀ (●), C₁₂ (■), and C₁₆ (▲) alkanes as a function of the number of methyl branches

Table 5 Predicted *Coelastrum* sp. biodiesel properties and specifications in US and European standards

Property (units)	TAP5	TAP15	TAP15-N	SWW5	SWW15	SWW15-N	ASTM 6751	EN 14214
ρ @ 15 °C (kg/m ³)	879.8	884.0	877.4	875.2	877.9	875.2		860–900
CN	55.3	52.4	57.0	58.8	56.6	60.8	47 min	51 min
ν @ 40 °C (mm ² /s)	4.2	3.9	4.3	4.4	4.2	4.1	1.9–6.0	3.5–5.0
HHV (MJ/kg)	39.8	39.6	39.8	39.8	39.7	39.6		
CFPP (°C)	−1.7	−6.4	1.9	3.2	2.3	18.7		
IV (g I/100 g biodiesel)	95.5	129.3	79.9	64.1	83.9	59.4		120 max
OSI (h)	4.0	4.2	4.2	4.3	4.4	7.9	3 min	6 min

biofuels. The yields, of both biomass and lipids, still need to be optimized to accomplish the viable commercial production of biofuels from microalgae. In order to accomplish this goal, it is required to know how the different metabolic pathways are affected by the variables studied in this work and to understand their interactions to better manipulate culture conditions towards the production of a certain biofuel. Finally, it is worth mentioning that optimization of the use of molasses as carbon and nitrogen source in microalgae culture is currently carried out in our group.

Funding Information The authors gratefully acknowledge the ASACONACYT financial support Grant No. 243145 for this project and CONACYT for María Guadalupe del Rayo Serrano-Vázquez scholarship No. 338220.

Glossary

ASTM	American Society of Testing Materials
BD	Biodiesel
BJ	Bio-jet fuel
EN	European Standards
E-T	Esterification + transesterification
FAME	Fatty acid methyl ester
FFA	Free fatty acids
FT-IR	Fourier transform infrared spectroscopy
GD	Green diesel
H	High quality
H/C	Hydrogen to oxygen atomic ratio
HC	Hydrocarbons
HC	Hydrocracking
HEFA	Hydrotreatment process for obtaining bio-jet fuel and green diesel
HI	Hydroisomerization
M	Medium quality
NIST	National Institute of Standards and Technology
NMX	Official Mexican Norm
PQ	Potential quality as product or feedstock
TLC	Thin layer chromatography

TG	Triglycerides
SWW	Synthetic wastewater

References

- Brännström H, Hemanathan K, Raimo A (2018) Current and potential biofuel production from plant oils. *Bioenergy Res* 11:592–613. <https://doi.org/10.1007/s12155-018-9923-2>
- Perez-García O, de-Bashan LE, Hernández JP, Bashan Y (2010) Efficiency of growth and nutrient uptake from wastewater by heterotrophic, autotrophic, and mixotrophic cultivation of *Chlorella vulgaris* immobilized with *Azospirillum brasilense*. *J Phycol* 46:800–812. <https://doi.org/10.1111/j.1529-8817.2010.00862.x>
- Abreu AP, Fernandes B, Vicente AA, Teixeira J, Dragone G (2012) Mixotrophic cultivation of *Chlorella vulgaris* using industrial dairy waste as organic carbon source. *Bioresour Technol* 118:61–66. <https://doi.org/10.1016/j.biortech.2012.05.055>
- Gaurav K, Srivastava R, Sharma JG, Singh R, Singh V (2016) Molasses-based growth and lipid production by *Chlorella pyrenoidosa*: a potential feedstock for biodiesel. *Int J Green Energy* 13(3):320–327. <https://doi.org/10.1080/15435075.2014.966268>
- Yan D, Lu Y, Chen YF, Wu Q (2011) Waste molasses alone displaces glucose-based medium for microalgal fermentation towards cost-saving biodiesel production. *Bioresour Technol* 102:6487–6493. <https://doi.org/10.1016/j.biortech.2011.03.036>
- Cheng Y, Lu Y, Gao C, Wu Q (2009) Algae-based biodiesel production and optimization using sugar cane as the feedstock. *Energy Fuel* 23:4166–4173. <https://doi.org/10.1021/ef9003818>
- Kang S, Fu J, Zhou N, Liu R, Peng Z, Xu Y (2018) Concentrated levulinic acid production from sugar cane molasses. *Energy Fuel* 32:3526–3531. <https://doi.org/10.1021/acs.energyfuels.7b03987>
- Teclu D, Tivchev G, Laing M, Wallis M (2009) Determination of the elemental composition of molasses and its suitability as carbon source for growth of sulphate-reducing bacteria. *J Hazard Mater* 161:1157–1165. <https://doi.org/10.1016/j.jhazmat.2008.04.120>
- Kim KH, Lee HY, Lee CY (2015) Pretreatment of sugarcane molasses and citric acid production by *Candida zeylanoides*. *Microbiol Biotechnol Lett* 43:164–168. <https://doi.org/10.4014/mbl.1503.03006>
- CONADESUC (2016) Melazas de caña de azúcar y su uso en la fabricación de dietas para ganado. https://www.gob.mx/cms/uploads/attachment/file/171888/Nota_Informativa_Noviembre_Melazas.pdf. Accessed 28 May 2019

11. Isleten-Hosoglu M, Gultepe I, Elibol M (2012) Optimization of carbon and nitrogen sources for biomass and lipid production by *Chlorella saccharophila* under heterotrophic conditions and development of Nile red fluorescence based method for quantification of its neutral lipid content. *Biochem Eng J* 61:11–19. <https://doi.org/10.1016/j.bej.2011.12.001>
12. Liu J, Huang J, Jiang Y, Chen F (2012) Molasses-based growth and production of oil and astaxanthin by *Chlorella zofingiensis*. *Bioresour Technol* 107:393–398. <https://doi.org/10.1016/j.biortech.2011.12.047>
13. Cai T, Park SY, Li Y (2013) Nutrient recovery from wastewater streams by microalgae: status and prospects. *Renew Sust Energ Rev* 19:360–369. <https://doi.org/10.1016/j.rser.2012.11.030>
14. Mousavi S, Najafpour GD, Mohammadi M, Seifi MH (2018) Cultivation of newly isolated microalgae *Coelastrum* sp. in wastewater for simultaneous CO₂ fixation, lipid production and wastewater treatment. *Bioprocess Biosyst Eng* 41:519–530. <https://doi.org/10.1007/s00449-017-1887-7>
15. Úbeda B, Gálvez JA, Michel M, Bartual A (2017) Microalgae cultivation in urban wastewater: *Coelastrum* cf. *pseudomicroporum* as a novel carotenoid source and a potential microalgae harvesting tool. *Bioresour Technol* 228:210–217. <https://doi.org/10.1016/j.biortech.2016.12.095>
16. Liu Z, Liu C, Hou Y, Chen S, Xiao D, Zhang J, Chen F (2013) Isolation and characterization of a marine microalga for biofuel production with Astaxanthin as a co-product. *Energies* 6:2759–2772. <https://doi.org/10.3390/en6062759>
17. Minillo A, Godoy HC, Fonseca GG (2013) Growth performance of microalgae exposed to CO₂. *J Clean Energy Technol* 1:110–114. <https://doi.org/10.7763/JOCET.2013.V1.26>
18. Hirose M, Mukaida F, Okada S, Noguchi T (2013) Active hydrocarbon biosynthesis and accumulation in a green alga *Botryococcus braunii* (race A). *Eukaryot Cell* 12:1132–1141. <https://doi.org/10.1128/EC.00088-13>
19. Herrera-Valencia VA, Us-Vázquez RA, Larqué-Saavedra FA, Barahona-Pérez LF (2012) Naturally occurring fatty acid methyl esters and ethyl esters in the green microalga *Chlamydomonas reinhardtii*. *Ann Microbiol* 62:865–870. <https://doi.org/10.1007/s13213-011-0361-z>
20. Santhakumaran P, Kookal S, Mathew L, Ray JG (2019) Bioprospecting of three rapid-growing freshwater green algae. *Bioresour Technol* 12:680–693. <https://doi.org/10.1007/s12155-019-09990-9>
21. Valdez-Ojeda R, González-Muñoz M, Us-Vázquez R, Narváez-Zapata J, Chavarria-Hernandez JC, López-Adrián S, Barahona-Pérez F, Toledano-Thompson T, Garduño-Solórzano G, Escobedo-Gracia Medrano RM (2015) Characterization of five fresh water microalgae with potential for biodiesel production. *Algal Res* 7:33–44. <https://doi.org/10.1016/j.algal.2014.11.009>
22. Nanduca HE (2015) Utilización de aguamiel de café y melaza en agua residual sintética en el cultivo de la microalga *Scenedesmus* sp para la producción de lípidos. M. Sc. Dissertation, Centro de Investigación Científica de Yucatán, Mexico
23. Harris EH (1989) The *Chlamydomonas* sourcebook, a comprehensive guide to biology and laboratory use. Academic, San Diego
24. Gorman DS, Levine RP (1965) Cytochrome f and plastocyanin: their sequence in the photosynthetic electron transport chain of *Chlamydomonas reinhardtii*. *Proc Natl Acad Sci U S A* 54:1665–1669. <https://doi.org/10.1073/pnas.54.6.1665>
25. Azianabiha AHK, Zahira Y, Siti RSA, Mohd ST (2016) Enhanced growth and nutrients removal efficiency of *Characium* sp. cultured in agricultural wastewater via acclimatized inoculum and effluent recycling. *J Environ Chem Eng* 4:3426–3432. <https://doi.org/10.1016/j.jece.2016.07.020>
26. Bligh EG, Dyer WJ (1959) A rapid method of total lipid extraction and purification. *Can J Biochem Physiol* 37:911–917. <https://doi.org/10.1139/o59-099>
27. Widjaja A, Chien CC, Hu YH (2009) Study of increasing lipid production from fresh water microalgae *Chlorella vulgaris*. *J Taiwan Inst Chem Eng* 40:13–20. <https://doi.org/10.1016/j.jtice.2008.07.007>
28. Pratas MJ, Freitas S, Oliveira MB, Monteiro SC, Lima AS, Coutinho JA (2010) Densities and viscosities of fatty acid methyl and ethyl esters. *J Chem Eng Data* 55:3983–3990. <https://doi.org/10.1021/je1012235>
29. Ramírez-Verduzco LF (2013) Density and viscosity of biodiesel as a function of temperature: empirical models. *Renew Sust Energ Rev* 19:652–665. <https://doi.org/10.1016/j.rser.2012.11.022>
30. Ramírez-Verduzco LF, Rodríguez-Rodríguez JE, del Rayo J-JA (2012) Predicting cetane number, kinematic viscosity, density and higher heating value of biodiesel from its fatty acid methyl ester composition. *Fuel* 91:102–111. <https://doi.org/10.1016/j.fuel.2011.06.070>
31. Knothe G (2002) Structure indices in FA chemistry. How relevant is the iodine value? *J Am Oil Chem Soc* 79:847–854. <https://doi.org/10.1007/s11746-002-0569-4>
32. Knothe G, Steidley KR (2005) Kinematic viscosity of biodiesel fuel components and related compounds. Influence of compound structure and comparison to petrodiesel fuel components. *Fuel* 84:1059–1065. <https://doi.org/10.1016/j.fuel.2005.01.016>
33. Pratas MJ, Freitas S, Oliveira MB, Monteiro SC, Lima AS, Coutinho JA (2011) Densities and viscosities of minority fatty acid methyl and ethyl esters present in biodiesel. *J Chem Eng Data* 56:2175–2180. <https://doi.org/10.1021/je1012235>
34. Freedman B, Bagby MO (1989) Heats of combustion of fatty esters and triglycerides. *J Am Oil Chem Soc* 66:1601–1605. <https://doi.org/10.1007/BF02636185>
35. Mishra S, Anand K, Mehta PS (2016) Predicting the cetane number of biodiesel fuels from their fatty acid methyl ester composition. *Energy Fuel* 30:10425–10434. <https://doi.org/10.1021/acs.energyfuels.6b01343>
36. Serrano M, Oliveros R, Sánchez M, Moraschini A, Martínez M, Aracil J (2014) Influence of blending vegetable oil methyl esters on biodiesel fuel properties: oxidative stability and cold flow properties. *Energy* 65:109–115. <https://doi.org/10.1016/j.energy.2013.11.072>
37. Park JY, Kim DK, Lee JP, Park SC, Kim YJ, Lee JS (2008) Blending effects of biodiesels on oxidation stability and low temperature flow properties. *Bioresour Technol* 99:1196–1203. <https://doi.org/10.1016/j.biortech.2007.02.017>
38. Zhan J, Hong Y HH (2016) Effects of nitrogen sources and C/N ratios on the lipid-producing potential of *Chlorella* sp. HQ. *J Microbiol Biotechnol* 26:1290–1302. <https://doi.org/10.4014/jmb.1512.12074>
39. Gao F, Yang H-L, Li C, Peng Y-Y, Lu M-M, Jin W-H, Bao J-J, Guo Y-M (2019) Effect of organic carbon to nitrogen ratio in wastewater on growth, nutrient uptake and lipid accumulation of a mixotrophic microalgae *Chlorella* sp. *Bioresour Technol* 282:118–124. <https://doi.org/10.1016/j.biortech.2019.03.011>
40. Chen F, Johns MR (1991) Effect of C/N ratio and aeration on the fatty acid composition of heterotrophic *Chlorella sorokiniana*. *J Appl Phycol* 3:203–209. <https://doi.org/10.1007/BF00003578>
41. Perez-García O, Bashan Y, Puente ME (2011) Organic carbon supplementation of sterilized municipal wastewater is essential for heterotrophic growth and removing ammonium by the microalga *Chlorella vulgaris*. *J Phycol* 47:190–199. <https://doi.org/10.1111/j.1529-8817.2010.00934.x>
42. Rai MP, Gupta S (2017) Effect of media composition and light supply on biomass, lipid content and FAME profile for quality biofuel production from *Scenedesmus abundans*. *Energy Convers*

- Manag 141:85–92. <https://doi.org/10.1016/j.enconman.2016.05.018>
43. Griffiths MJ, van Hille RP, Harrison STL (2014) The effect of degree and timing of nitrogen limitation on lipid productivity in *Chlorella vulgaris*. Appl Microbiol Biotechnol 98:6147–6159. <https://doi.org/10.1007/s00253-014-5757-9>
44. El-Sheekh MM, Bedaiwy MY, Osman ME, Ismail MM (2014) Influence of molasses on growth, biochemical composition and ethanol production of the green algae *Chlorella vulgaris* and *Scenedesmus obliquus*. Journal of Agricultural Engineering and Biotechnology 2:20–28. <https://doi.org/10.18005/JAEB0202002>
45. Figueroa GM, Pittman JK, Theodoropoulos C (2017) Kinetic modelling of starch and lipid formation during mixotrophic, nutrient-limited microalgal growth. Bioresour Technol 241:868–878. <https://doi.org/10.1016/j.biortech.2017.05.177>
46. Gifuni I, Olivieri G, Pollio A, Marzocchella A (2018) Identification of an industrial microalgal strain for starch production in biorefinery context: the effect of nitrogen and carbon concentration on starch accumulation. New Biotechnol 41:46–54. <https://doi.org/10.1016/j.nbt.2017.12.003>
47. Yao LX, Gerde JA, Lee SL, Wang T, Harrata KA (2015) Microalgae lipid characterization. J Agric Food Chem 63:1773–1787. <https://doi.org/10.1021/jf5050603>
48. Frassanito R, Cantonati M, Tardio M, Mancini I, Guella G (2005) On-line identification of secondary metabolites in freshwater microalgae and cyanobacteria by combined liquid chromatography-photodiode array detection-mass spectrometric techniques. J Chromatogr A 1082:33–42. <https://doi.org/10.1016/j.chroma.2005.02.066>
49. Meng X, Pan Q, Ding Y, Jiang L (2014) Rapid determination of phospholipid content of vegetable oils by FTIR spectroscopy combined with partial least-square regression. Food Chem 147:272–278. <https://doi.org/10.1016/j.foodchem.2013.09.143>
50. Linstrom PJ, Mallard WG (2018) NIST chemistry webbook, NIST Standard Reference Database Number 69. <https://webbook.nist.gov/chemistry/>. Accessed 28 May 2019
51. Taylor RJ, Petty RH (1994) Selective hydroisomerization of long chain normal paraffins. Appl Catal A Gen 119:121–138. [https://doi.org/10.1016/0926-860X\(94\)85029-1](https://doi.org/10.1016/0926-860X(94)85029-1)
52. Calemma V, Peratello S, Perego C (2000) Hydroisomerization and hydrocracking of long chain n-alkanes on Pt/amorphous SiO₂-Al₂O₃ catalyst. Appl Catal A Gen 190:207–218. [https://doi.org/10.1016/S0926-860X\(99\)00292-6](https://doi.org/10.1016/S0926-860X(99)00292-6)
53. López-Rosales AR, Ancona-Canché K, Chavarria-Hernandez JC, Barahona-Pérez F, Toledano-Thompson T, Garduño-Solórzano G, López-Adrian S, Canto-Canché B, Polanco-Lugo E, Valdez-Ojeda R (2019) Fatty acids, hydrocarbons and terpenes of *Nannochloropsis* and *Nannochloris* isolates with potential for bio-fuel production. Energies 12:130. <https://doi.org/10.3390/en12010130>
54. Wang WC, Tao L (2016) Bio-jet fuel conversion technologies. Renew Sust Energ Rev 53:801–822. <https://doi.org/10.1016/j.rser.2017.04.058>

Publisher's Note Springer Nature remains neutral with regard to jurisdictional claims in published maps and institutional affiliations.